Available online at www.sciencedirect.com

ScienceDirect

Procedia Environmental Sciences 32 (2016) 221 – 229

Procedia Environmental Sciences

International Conference – Environment at a Crossroads: SMART approaches for a sustainable future

Comparison of Multi-Temporal Differential Interferometry Techniques Applied to the Measurement of Bucharest City Subsidence

Mihaela Gheorghe[a]*, Iuliana Armaş[b]

[a]*Technical University of Civil Engineering of Bucharest, Faculty of Geodesy, Bucharest, Romania, Email: mihaela.gheorghe@utcb.ro*
[b]*University of Bucharest, Faculty of Geography, Department of Geomorphology-Pedology-Geomatics, NicolaeBalcescu 1, Sector 1, 010041, Bucharest, Romania , Email:iulia_armas@geo.unibuc.ro*

Abstract

This paper aims to present some of the most popular multi-temporal differential interferometry (DInSAR) techniques that are used for monitoring surface deformations in different types of areas. We focus on the urban area of Bucharest, where we applied the PS (Persistent Scatterers) and SBAS (Small BAseline Subset) techniques. The PS approach analyzes interferograms generated with a common master image, looking at point targets that remain stable over time, generating signal that remains coherent from an acquisition to another. The SBAS approach relies on small baseline interferograms that maximize the spatial and temporal coherence. In this paper we compare these techniques by applying them to the urban area of Bucharest using TSX data. . Both PS and SBAS methods generate millimetre ground displacement rates. The PS subsidence values range from -22 mm/yr to 22 mm/yr while the SBAS value rates are lower, from -10 mm/yr to 10 mm/yr. The subsidence rate maps are compared from a quantitative and qualitative point of view, taking into account also the type of movements that the techniques can derive. The current paper is mainly methodological oriented, aiming to present the PS and SBAS techniques in a comparative way. Less emphasis is put on the initial results, which are presented briefly in order to give an insight about further study directions.

Peer-review under responsibility of the organizing committee of ECOSMART 2015

Keywords: DInSAR; PS, SBAS, subsidence

* Corresponding author. Tel.: +40766704411;
E-mail address: mihaela.gheorghe@geodezie.utcb.ro

Peer-review under responsibility of the organizing committee of ECOSMART 2015
doi:10.1016/j.proenv.2016.03.027

1. Introduction

Due to its capacity to provide extensive and up-to-date geospatial information, remote sensing becoming an important technology for natural hazards management. Data fusions between optical, radar and thermal imagery can play a role in each of the four phases of disaster management cycle (mitigation, preparedness, response and recovery) [1] for hazards like earthquakes, volcanic eruptions, flooding or landslides. Optical, thermal and microwave data have been used for detection of earthquakes and faulting, [2, 3, 4], volcanic activity [5, 6, 7, 8, 9], landslides [10, 11, 12, 13] and flooding [14, 15, 16].

Ground subsidence represents another type of hazard that is evolving during a large time scale, being characterized by smaller but consistent changes. Ground subsidence manifests more frequently in urban and peri-urban areas, being triggered various causes such as water exploitation or mining [17]. The subsidence rate in urban areas can influence the flooding risk and cause infrastructure damages through ground fractures [18]. Therefore, we consider that subsidence is a phenomenon that should receive the same importance as the other mentioned hazards. Most important application of remote sensing for urban environments is assessing the extent of damages suffered by an area affected by hazards, and monitoring its recovery. In urban areas the damage assessment is done by interpreting the degree of building damage, flood levels or ground movements in case of earthquakes and landslides. The downside of using optical imagery for damage assessment in urban zones is that the affected areas are identified mainly through manual interpretation [19, 20]. This type of application depends on user's experience and can be subject of interpretation errors.

A faster and more accurate detection of the affected infrastructure or ground motions due to hazards would require a change in spectral reflectance that can be depicted automatically. But in most cases, changes that affect the buildings structure cannot be identified by means of spectral information. Better results were obtained by Stramondo et al., (2006)[3] through image differencing of multi-date spectral ratios of multi-temporal optical and Synthetic Aperture Radar (SAR) imagery to detect building debris after earthquakes in Iran and Turkey. SAR data can be used to measure changes in topography and building damages through multi-temporal analysis of pre and post disaster imagery [21]. However this technique is limited by the significant variance of the backscatter intensity of different areas and dependence on incidence angle [1].

When it comes to mapping ground deformations, Differential SAR interferometry is considered one of the best available techniques. DInSAR calculates the phase difference between images acquired at different times, before and after an event [22, 23]. Phase difference is an indicator of the degree of change suffered by an area between two acquisitions. Phase decorrelation can be caused by different surface condition between two acquisitions, different atmospheric conditions or large spatial baselines. The accuracy of this technique depends therefore on many parameters, like ground and atmospheric conditions, wave-band and backscatter intensity. With an accuracy better than a quarter of SAR wavelength, the techniques is suitable for mapping ground deformations caused by moderate earthquakes and landslides, or identifying building debris and large displacements through decorrelation between acquisitions.

Considering all possible parameters that can influence phase changes between acquisitions, and the small order of magnitude for displacement values, the aim of this paper is to investigate how two different multi-temporal DInSAR techniques can emphasize complementary data about Bucharest study area. The two techniques that we apply are Permanent Scatterer and Small BAseline Subset interferomtery.

The test area is Bucharest, the capital of Romania and the largest city from the country with a population of approximately 2 million inhabitants. Bucharest is found in the South-Eastern part of the country, the Bucharest area is located in the Romanian Plain between the Carpathian Mountains in the North and the Danube River in the South, on the foreland basin of the Carpathian Mountains. The near-surface geology is represented by up to 300 m thick layering of Quaternary poorly-consolidated fluvial and lacustrine deposits. The plain landscape was shaped through fluvial processes determined by two small rivers: the Dâmboviţa, and its left side affluent, Colentina.

Main hazards affecting Bucharest's area are earthquakes and subsidence. Ground subsidence values are not critical, but they may influence the seismic response of the urban area. Bucharest's area is also characterized by a weak intensity of signal backscatter, indicating low rates of displacements.

In the following sections we present a comparison between the mentioned techniques regarding principles and data processing steps, and a short insight on our initial results obtained for a dataset of TSX images covering

Bucharest area. In the end we discuss and conclude regarding the importance of using different InSAR methods, based on the characteristics of the study area.

1. Differential InSAR multi-temporal techniques

Differential Synthetic Aperture Radar interferometry, or DInSAR, represents a microwave remote sensing technique that can be used to determine surface deformations in the line of sight (LOS) direction of a sensor, by pairing SAR images of the same scene acquired at different times. The image pairs are named interferograms [24]. The first studies using differential interferometry were analyzing single pairs to determine changes that occurred in an area between two acquisition dates [25, 26]. Later, the technique was adapted to a multi-temporal approach that allows monitoring surface deformations in time, by exploiting sets of interferograms obtained from large sequences of SAR images of the study area [8, 27, 28, 29]. The most widely used methods are the Permanent Scatterer and Small BAseline Subset which we describe and compare in the following sections.

1.1. The Persistent Scatterer technique

The interferometric phase is influenced by a series of signals like the satellite-target relative position, temporal changes in the scene or atmospheric fluctuations. The Persistent Scatterer Technique was first proposed by Ferretti et al. (2001)[29] to overcome the limitations of SAR interferometry, often affected by temporal, atmospheric or geometrical decorrelation in surface monitoring related applications. The method is based on identifying stable reflectors in the multi-temporal interferometric SAR scenes. The stable reflectors have been named Permanent (or persistent) scatterers and are exploited for obtaining millimetre crust deformations and improved DEM accuracies (submeter level). Ferretti et al., (2000)[27] and Ferretti et al., (2001)[29] proposed an amplitude dispersion index for identifying these PS candidates. Because this index can be applied only for large data stacks, Berardino et al., (2002)[8] proposed using a coherence stability indicator. The persistent scatterers are natural or man-made objects that present a stable signal phase from an acquisition to another, displaying a high coherence over a SAR data stack.

1.2. The Small BAseline Subset technique

The basic principle of this technique consists in a suitable combination of multiple interferograms with corresponding small baselines. The resulted small baseline interferograms are implemented in a linear model where the combination of small baseline depends on the vector containing values of the unwrapped differential interferometric phase [30]. By solving the linear model, the sampling rate of the method is increased, while phase noise is reduced and backscatter preserved by choosing a coherence threshold. Like in the case of the PS method, only coherent pixels are exploited, but in the SBAS technique the values of the coherent pixels are interpolated over larger areas using Delaunay triangulation as described by Rosen and Costantini, (1999)[31].

1.3. Comparison between the PS and SBAS algorithms

In this paper we present a summary of the PS and SBAS techniques steps with the corresponding algorithm in order to emphasize the differences between the methods that make the subject of this paper. In general we tried to keep the notations from the original literature, but for the purpose of comparing the two methods we also adapted notations where needed. However, the technique steps described below are based on the initial PS presented by Ferretti et al., (2000)[27] and on the description of the SBAS algorithm given by Berardino et al., (2002)[8] and Lanari et al., (2004)[28].

- *Full-resolution interferogram formation*: Both PS and SBAS algorithms consider a set of $N+1$ SAR images of the same scene consecutively $(t_0, .., t_N)$. In the case of PS, from the $N+1$ SAR images a number of N interferograms are obtained by pairing each slave image, *IS*, with a reference master image, *IE*. The expression of the phase difference between a slave image and the master image for a pixel $\underline{\mathbf{x}}$ of a generic focused SAR image:

$$\varphi_n(\underline{x}) = \psi_{IS_n}(\underline{x}) - \psi_{IE}(\underline{x}); n = 1,..,N; \quad (1)$$

By applying the SBAS algorithm, from *N+1* SAR images are generated *M* interferograms that respect the constraints referring to the maximum temporal and spatial baselines mentioned above. Because more than one master image is used, we define two index vectors related to the master and slave time acquisitions:

$$IS = [IS_1,..,IS_M];\ IE = [IE_1,..,IE_M]; \quad (2)$$

The phase expression for a pixel in an interferogram becomes in this case:

$$\varphi_m(\underline{x}) = \psi_{IE_m}(\underline{x}) - \psi_{IE_m}(\underline{x}); m = 1,..,M; \quad (3)$$

- *Interferometric process:*

a) *Co-registration* is the process of superimposing more SAR images with the same acquisition geometry specific to the PS technique. During this process it is possible for the images with different pixel size to require resampling. All images are coregistered to the geometry of the master image*;*

b) *Differential interferograms formation and flattening*. The difference in distance from a point on the Earth and sensor that occurs between two acquisitions can be determined by the phase difference between two complex SAR images. In both techniques, differential interferograms are obtained by using a reference digital elevation model (DEM) that can be either generated from tandem SAR image pairs or come from an external source. The DEM helps remove the topographic phase from the initial interferograms. The best elevation accuracy can be obtained a combination between a multi-interferogram DEM and one obtained with different accurate techniques (stereomodel obtained from SPOT imagery) [32];

c) *Filtering and coherence generation:* Specific to the SBAS technique, it generates an interferogram with reduced phase noise. By filtering it is obtained also the interferometric coherence, which indicates the phase quality. In literature have been used mainly three filtering techniques: the Adaptive, Boxcar and Goldstein filters [33, 34];

d) *Phase unwrapping* is the process that resolves the phase ambiguity which appears when applying the SBAS technique, each time the phase difference of an interferogram becomes larger than 2π. The phase ambiguity occurs because the phase difference of an interferogram can only hav a value that is modulo 2π [35];

Between the interferometric process and the first inversion step that is specific to both techniques, the SBAS technique also effectuates an orbital refinement and a re-flattening on all flattened interferometric pairs obtained at the preceding point.

- *First Inversion:* this step implies deriving the residual height and the displacement velocity. For the PS technique it is identified a number of “coherent radar signal reflectors” (Persistent Scatterers). Once these targets are identified, their phase history is analyzed and good PS candidates are selected. Usually good PS candidates are the majority of man-made structures or natural rock formations. These candidates need to be stable in time and oriented conveniently in the SAR sensor’s direction. By using the identified scatterers, the PS technique removes the influences of the atmosphere. In the SBAS algorithm, the first inversion consists in flattening the complex interfergrams, repeating the phase unwrapping and the orbital refinement with the goal of improving the quality of the obtained products. The PS technique uses only a linear model in the first inversion, while the SBAS technique gives the possibility of using also quadratic and cubic models to generate acceleration and acceleration variation besides height and displacement velocity [8].

- *Second Inversion:* This step uses the products obtained in the first inversion to estimate the components of the atmospheric influence. In the case of the PS, the products from the previous step are the ones obtained from applying the linear model. For the SBAS technique, these products are represented by unwrapped products. The second inversion derives the displacement time series from which the atmospheric influence is removed. The displacement model that is fitted in the end after removing the phase components is again a linear model in the case of PS and a linear, a quadratic or a cubic model in the SBAS algorithm. For both techniques the influence of the atmosphere is corrected by using a low pass and a high pass filter. The low pass component of the atmosphere accounts for the spatial distribution of the variations while the high pass component is represented by the temporal distributions.

2. Data processing and results

In this section we describe a few steps and parameters that we used to apply PS and SBAS algorithms to obtain deformation time-series resulted from processing 27 SAR acquisitions over Bucharest. The data has been acquired between March 2011 and December 2014 in ascending and descending passes of TerraSAR-X satellite. All data was processed using Sarmap's software, Sarscape.

The InSAR pairs selected for the PS algorithm were referenced to a master acquisition from 26th of June, 2012. For the SBAS algorithm, the pairs had a perpendicular base of less than 500 m and a temporal baseline of less than 2 years. With these considerations we obtained a number of 26 interferograms for the PS algorithm and 178 for the SBAS algorithm. The influence of topography was removed by using an external DEM, SRTM-X, available from DLR [36]. The processing steps, the results and their interpretation will be presented in detail in a further paper.

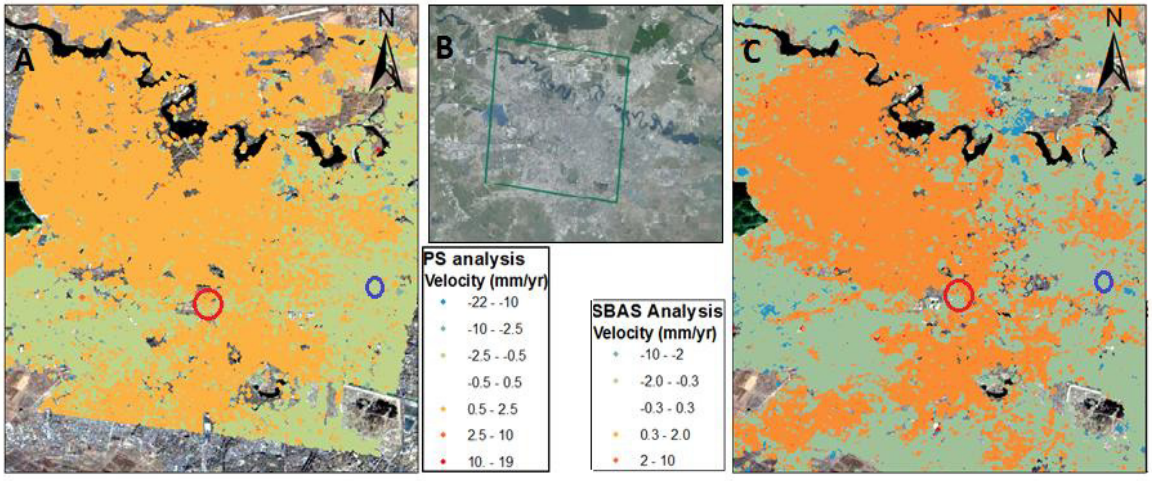

Fig. 1. (A) Map representing the average velocity obtained from PS processing of SAR images between 2011 and 2014 in the centre of Bucharest. (B) Extent of the area that was processed using the PS and SBAS techniques. (C) Map representing the average velocity obtained from SBAS processing of SAR images between 2011 and 2014 in the centre of Bucharest. The red and the blue extents delimitate an uplifting and a subsiding area respectively.

The velocity of the surface movement determined from PS InSAR measurements varies from approimately -22 mm/yr to 22, while the velocity shown by the SBAS results is lower, ranging from around -10 to 10 mm/yr . In both cases, there are few to no points in vegetated areas like parks. For the same area of the city centre, the PS method returned considerably less points than the SBAS processing, although urban areas are usually known to contain a large number of PS points. Regarding the movement patterns, we can identify both uplifting and subsidence trends throughout the city, with movements that differentiate the limits of Dâmbovița's riverbed, and other areas that are

believed to be affected by geological processes that need to be further investigated.

The deformations depicted for the city centre (Fig. 2 (B)) by the two methods indicate the same pattern of displacements (with subsiding and uplifting areas) (Fig. 2 (A), (C)). Although the pattern of displacement indicated by the two sets of results is similar, the average velocity values calculated with PS tend to be higher than the ones obtained when applying the SBAS technique. When we select pixels from uplifting areas (Fig. 2.) and subsiding areas (Fig.3.) and represent their behaviour in time through displacement time series, we can observe that the SBAS results show a clearer tendency curve than the PS. This type of results indicates that the PS results are more affected by noise while the SBAS is able to mitigate it by imposing spatial and temporal constraints on the selection of the interferograms.

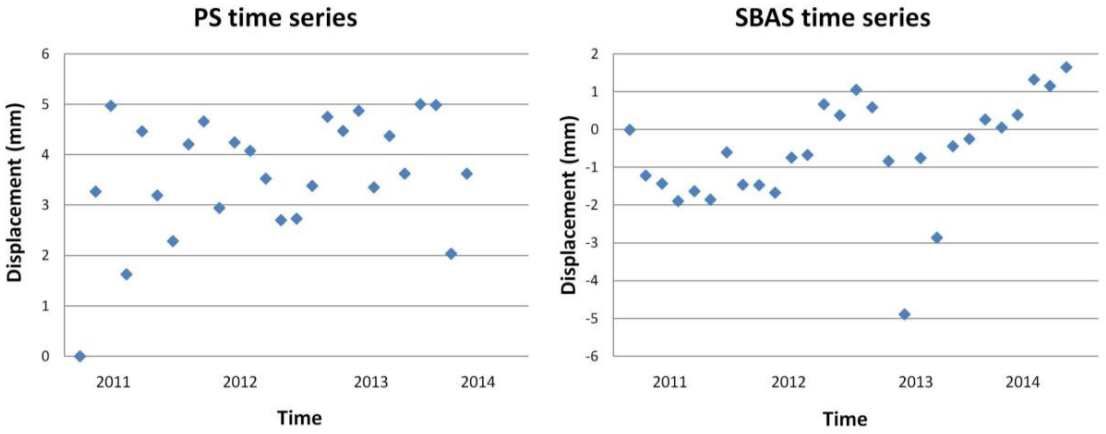

Fig. 2. Displacement time series depicted for an uplifting area (red circle in Fig.1.)

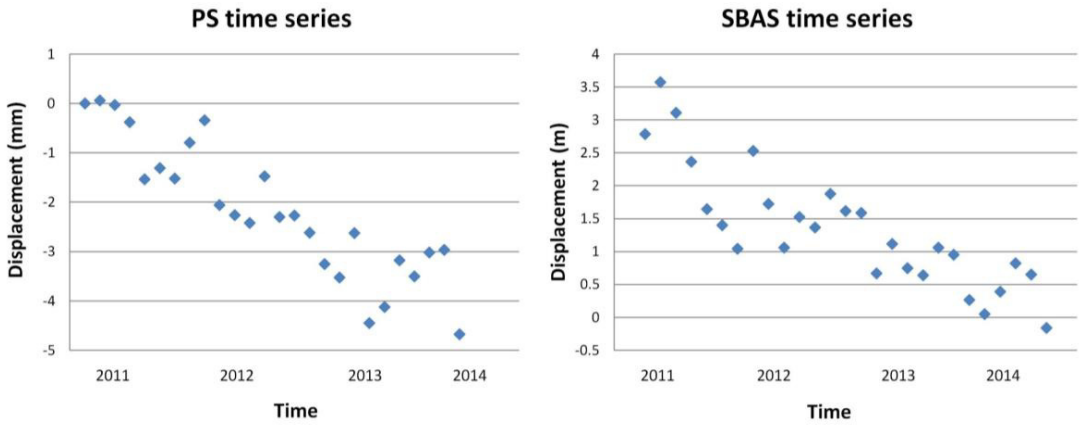

Fig.3. Displacement time series depicted for a subsiding area (blue circle in Fig 1.)

3. Discussion

The main difference between the two techniques is the method of selecting radar targets with reliable phase measurements. The PS technique uses a master image to which all the other acquisitions are referenced, while the SBAS technique selects convenient master-slave pairs with temporal and geometric baselines that maximize the coherence. The PS interferograms are analyzed at single look resolution in order to identify dominant scatterers within cells. The resolution cells that contain a dominant scatterer will display an increased signal to noise ratio. Instead of looking at single cells, the SBAS method looks for the highly correlated areas. Usually in this case multi-looked interferograms are preferred, since they improve the phase estimates and reduce the speckle while also reducing the data volume. Since PS looks at point data and SBAS identifies coherent areas, it can be said that the SBAS method cannot "see" small radar targets as the PS does, while the PS is more likely to be affected by noise over large areas. The differences that characterize the algorithms can be identified in the obtained results. By applying both techniques, we obtained the same coherent areas and same displacement patterns, with slightly different velocity values for individual points.

The findings of Lauknes et al., (2006)[30], who compared subsidence values in Oslo by applying PS and SBAS methods using ERS 1/2 data, agree with our results regarding more noise affecting PS results, but similar pattern areas and subsidence tendency. The average velocity values resulted from the SBAS analysis in this study is of 5 mm/yr, which is slightly larger than the average velocity we determined for Bucharest. There are also other studies, like the one of Rao et al., (2012)[37], who focused on landslides in Himalayan regions using both InSAR methods, but found considerably differences between the SBAS and PS results, especially for the ascending pass of the ENVISAT ASAR satellite. While the first study shows low average velocity values that are comparable to the ones we depicted, the study of Rao et al., (2012)[37] shows a larger velocity value interval, from -38 mm/yr to 38 mm/yr. Another difference between our results and this study is represented by the number of coherent points that are determined using each method. Unlike our results, where PS points are considerably less than SBAS points, in the case of landslide studies the authors found less SBAS points because of using coherent areas in a highly dynamic area. When applying PS and SBAS techniques to studying subsidence in urban area, other studies, like those of Lauknes et al., (2006)[30] and Yan et al., (2012)[38], describe obtaining considerably more coherent points in the case of SBAS than of PS.

The differences that exist between the methods make them applicable in various types of applications. For example, the PS is more suitable for studying infrastructure behavior. Because the radar targets are discrete objects we can analyze them at an individual level. The SBAS, on the other side, can be used in geological studies interested in long time behavior of the earth surface. Another aspect that recommends the SBAS method for geological studies is that the algorithm can depict nonlinear movement due to the modeling that it applies in the inversion steps. The PS only applies a linear model to determine the velocity and displacement values over time.

4. Conclusion

In the current paper we compared two algorithms from a theoretical point of view and presented an initial set of results that emphasizes the differences between them. With an average velocity of -2 mm/yr to 2 mm/yr for PS and -1.6 to 1.6 for SBAS analysis, these values do not indicate an extreme case of subsidence in Bucharest, but a further study will analyze the movement patterns and velocity trends from a geological point of view. We already mentioned that we would consider the SBAS analysis more suitable for a geological study, due to maximized coherence over large areas and noise mitigation. Also the possibility of depicting non-linear movements that usually characterize long-term geological patterns makes it a more suitable technique for the purpose of this type of studies. Regardless the object of a further study, the possibility of processing the same dataset with two different methods and obtaining two complementary result datasets makes SAR images a valuable material basis that can be exploited. Thus, by improving the understanding and application of PS-SBAS techniques, we will better quantification human-environment interactions, land resource utilization and resource conflicts between urbanization and ecosystem services, physical processes associated with natural hazards like earthquakes, landslides, etc., as well as the relationship between the deep Earth interior and shallow geodynamic processes.

Acknowledgements

This research was financed by grant 285/2011 of the Romanian National Authority for Scientific Research and grant 78/29.11.2013 with the Romanian Space Agency. TSX data were provided via DLR Proposal LAN 1444 entitled “Ground Subsidence in Bucharest, Romania based on Historical and Recent Data.”

References

1. Joyce KE, Belliss SE, Samsonov SV, McNeill SJ, Glassey PJ. A review of the status of satellite remote sensing and image processing techniques for mapping natural hazards and disasters. *Progress in Physical Geography*; 2009.
2. Ryder I, Parsons B, Wright TJ, Funning GJ. Post-seismic motion following the 1997 Manyi (Tibet) earthquake: InSAR observations and modelling. *Geophysical Journal International*. 2007;169(3):1009-27.
3. Stramondo S, Bignami C, Chini M, Pierdicca N, Tertulliani A. Satellite radar and optical remote sensing for earthquake damage detection: results from different case studies. *International Journal of Remote Sensing*. 2006;27(20):4433-47.
4. Choudhury S, Dasgupta S, Saraf AK, Panda S. Remote sensing observations of pre-earthquake thermal anomalies in Iran. International Journal of Remote Sensing. 2006;27(20):4381-96.
5. Ji L, Lu Z, Dzurisin D, Senyukov S. Pre-eruption deformation caused by dike intrusion beneath Kizimen volcano, Kamchatka, Russia, observed by InSAR. *Journal of Volcanology and Geothermal Research*. 2013;256:87-95.
6. Watson IM, Realmuto VJ, Rose WI, Prata AJ, Bluth GJ, Gu Y, Bader CE, Yu T. Thermal infrared remote sensing of volcanic emissions using the moderate resolution imaging spectroradiometer. *Journal of volcanology and geothermal research*. 2004;135(1):75-89.
7. Piscini A, Picchiani M, Chini M, Corradini S, Merucci L, Del Frate F, Stramondo S. A neural network approach for the simultaneous retrieval of volcanic ash parameters and SO2 using MODIS data. *Atmos. Meas. Tech. Discuss*.. 2014;7:3349-95.
8. Berardino P, Fornaro G, Lanari R, Sansosti E. A new algorithm for surface deformation monitoring based on small baseline differential SAR interferograms. *Geoscience and Remote Sensing, IEEE Transactions* on. 2002 Nov;40(11):2375-83.
9. Hooper A, Zebker H, Segall P, Kampes B. A new method for measuring deformation on volcanoes and other natural terrains using InSAR persistent scatterers. *Geophysical research letters*. 2004;31(23).
10. Necsoiu M, McGinnis RN, Hooper DM. New insights on the Salmon Falls Creek Canyon landslide complex based on geomorphological analysis and multitemporal satellite InSAR techniques. Landslides. 2014;11(6):1141-53.
11. Greif V, Vlcko J. Monitoring of post-failure landslide deformation by the PS-InSAR technique at Lubietova in Central Slovakia. Environmental Earth Sciences. 2012;66(6):1585-95.
12. Pradhan B, Lee S. Landslide susceptibility assessment and factor effect analysis: backpropagation artificial neural networks and their comparison with frequency ratio and bivariate logistic regression modelling. Environmental Modelling & Software. 2010 Jun 30;25(6):747-59.
13. Mondini AC, Guzzetti F, Reichenbach P, Rossi M, Cardinali M, Ardizzone F. Semi-automatic recognition and mapping of rainfall induced shallow landslides using optical satellite images. Remote Sensing of Environment. 2011; 115(7):1743-57.
14. Townsend PA, Walsh SJ. Modeling floodplain inundation using an integrated GIS with radar and optical remote sensing. Geomorphology. 1998; 21(3):295-312.
15. Townsend PA. Mapping seasonal flooding in forested wetlands using multi-temporal Radarsat SAR. Photogrammetric engineering and remote sensing. 2001; 67(7):857-64.
16. Gaurav K, Sinha R, Panda PK. The Indus flood of 2010 in Pakistan: a perspective analysis using remote sensing data. Natural hazards. 2011;59(3):1815-26.
17. Foster SS, Lawrence A, Morris B. Groundwater in urban development: assessing management needs and formulating policy strategies. *World Bank Publications*; 1998.
18. Cabral-Cano E, Dixon TH, Miralles-Wilhelm F, Díaz-Molina O, Sánchez-Zamora O, Carande RE. Space geodetic imaging of rapid ground subsidence in Mexico City. *Geological Society of America Bulletin*. 2008;120(11-12):1556-1566.
19. Fu B, Ninomiya Y, Lei X, Toda S, Awata Y. Mapping active fault associated with the 2003 Mw 6.6 Bam (SE Iran) earthquake with ASTER 3D images. *Remote Sensing of Environment*. 2004;92(2):153-7.
20. Walker RT. A remote sensing study of active folding and faulting in southern Kerman province, SE Iran. *Journal of Structural Geology*. 2006;28(4):654-68.
21. Matsuoka M, Yamazaki F. Building damage mapping of the 2003 Bam, Iran, earthquake using Envisat/ASAR intensity imagery. *Earthquake Spectra*. 2005; (S1):285-94.
22. Massonnet D, Feigl KL. Radar interferometry and its application to changes in the Earth's surface. *Reviews Of Geophysics-Richmond Virginia Then Washington-*. 1998: 36:441-500.
23. Casu F, Manzo M, Lanari R. A quantitative assessment of the SBAS algorithm performance for surface deformation retrieval from DInSAR data. *Remote Sensing of Environment*. 2006;102(3):195-210.
24. Gabriel AK, Goldstein RM, Zebker HA. Mapping small elevation changes over large areas: differential radar interferometry. *Journal of Geophysical Research: Solid Earth* (1978–2012). 1989 ;94(B7):9183-91.
25. Massonnet D, Rossi M, Carmona C, Adragna F, Peltzer G, Feigl K, Rabaute T. The displacement field of the Landers earthquake mapped by radar interferometry. *Nature*. 1993;364(6433):138-42.
26. Rosen PA, Hensley S, Zebker HA, Webb FH, Fielding EJ. Surface deformation and coherence measurements of Kilauea Volcano, Hawaii, from SIR-C radar interferometry. *Journal Of Geophysical Research-All Series-*. 1996;101:23-109.

27. Ferretti A, Prati C, Rocca F. Nonlinear subsidence rate estimation using permanent scatterers in differential SAR interferometry. *Geoscience and Remote Sensing, IEEE transactions on*. 2000; 38(5):2202-12.
28. Lanari R, Mora O, Manunta M, Mallorquí JJ, Berardino P, Sansosti E. A small-baseline approach for investigating deformations on full-resolution differential SAR interferograms. *Geoscience and Remote Sensing, IEEE Transactions on*. 2004; 42(7):1377-86.
29. Ferretti A, Prati C, Rocca F. Permanent scatterers in SAR interferometry. *Geoscience and Remote Sensing, IEEE Transactions on*. 2001; 39(1):8-20.
30. Lauknes TR, Dehls J, Larsen Y, Høgda KA, Weydahl DJ. A comparison of SBAS and PS ERS InSAR for subsidence monitoring in Oslo, Norway. In *Fringe 2005 Workshop* 2006 Feb (Vol. 610, p. 58).
31. Rosen PA, Costantini M. A generalized phase unwrapping approach for sparse data. In *Proceedings of IGARSS* 1999 Jun (Vol. 28).
32. Ferretti A, Prati C, Rocca F. Multibaseline InSAR DEM reconstruction: The wavelet approach. *Geoscience and Remote Sensing, IEEE Transactions on*. 1999;37(2):705-15.
33. Fornaro G, Guarnieri AM. Minimum mean square error space-varying filtering of interferometric SAR data. *Geoscience and Remote Sensing, IEEE Transactions on*. 2002;40(1):11-21.
34. Ghulam A, Amer R, Ripperdan R. A filtering approach to improve deformation accuracy using large baseline, low coherence DInSAR phase images. *In Geoscience and Remote Sensing Symposium (IGARSS)*, 2010 Jul 25 (pp. 3494-3497).
35. Reigber A, Moreira J. Phase unwrapping by fusion of local and global methods. *In Geoscience and Remote Sensing, 1997. IGARSS'97. Remote Sensing-A Scientific Vision for Sustainable Development.*, 1997 Aug 3 (Vol. 2, pp. 869-871).
36. SRTM-X (2011). Elevation models from SRTM now available for download free of charge http://www.dlr.de/dlr/en/desktopdefault.aspx/tabid -10212/332_read-817/
37. Rao YS, Ojha C, Deo R. Application of persistent scatterer interferometry for identification of landslide areas of Himalayan region. In Geoscience and Remote Sensing Symposium (IGARSS), 2012 IEEE International, 2012 Jul 22 (pp. 3851-3854).
38. Yan Y, Doin MP, López-Quiroz P, Tupin F, Fruneau B, Pinel V, Trouvé E. Mexico city subsidence measured by InSAR time series: Joint analysis using PS and SBAS approaches. Selected Topics in *Applied Earth Observations and Remote Sensing, IEEE Journal of. 2012 Aug;5*(4):1312-26.